UNIVERSITY OF
FLORIDA

Department of Aerospace Engineering,
Mechanics & Engineering Science

231 Aerospace Building
PO Box 116250
Gainesville FL 32611-6250
Tel: (352) 392-0961
Fax: (352) 392-7303

October 4, 1999

Dr. Jonathan B. Ransom
Analytical and Computational Methods Branch
Structures and Materials
Mail Stop 240
NASA Langley Research Center
Hampton, VA 23681-2199

Dear Dr. Ransom:

Enclosed please find the final report for NAG-1-2060. We apologize for any inconvenience caused by our delay. Please contact me at the phone number or e-mail address above if additional information is required. Thank you.

Sincerely,

Janis C. Machnik
Grants Specialist

Enclosure

cc: NASA Center for AeroSpace Information (CASI)
LaRC Grant Officer
ONR Admin Grants Officer
A. Kurdila

Wavelet and Multiresolution Analysis for Finite Element Networking Paradigms
NAG-1-2060

Final Report

prepared by

Andrew J. Kurdila, Principal Investigator
University of Florida
Department of Aerospace Engineering,
Mechanics and Engineering Science
Gainesville, Florida 32611-6250
(352) 392-0961

Robert C. Sharpley
Department of Mathematics
University of South Carolina
Columbia, South Carolina

Grant Office Contact:

Janet E. Chitty
POB 116550
University of Gainesville
Gainesville, FL 32611
(352) 392-9448

prepared for

Jonathon Ransom
NASA Langley Research Center

Discussions concerning the technical aspects of this proposal
have been held with

Dr. Jerrold Housner
NASA Langley Research Center

Background:

This program of research was initiated with the submission in June 10, 1997 of the proposal entitled

"Wavelet and Multiresolution Analysis for Finite Element Networking Paradigms,"

The original starting date for the proposal was suggested as July 14, 1997. Nearly 11 months later, on 5/1/98, the project was initiated with an award of $20,000 that was split between researchers at the University of Florida and the University of South Carolina. The original statement of work in the proposal called for

> "... a focused plan of research... to extend [the authors] recent contributions to multiresolution and wavelet analysis to derive, develop and implement:
>
> (i) wavelet based methodologies for the compression, transmission, decoding, and visualization of three dimensional finite element geometry and simulation data in a network environment,
> (ii) methodologies for interactive algorithm monitoring and tracking in computational mechanics, and
> (iii) methodologogies for interactive algorithm steering for the acceleration of large scale finite element simulations."

The original budget for the above statement of work was $252,200. During the contractual period, the project monitor Dr. Jerrold Housner moved to a different position at NASA Langley Research Center, and the project ceased to be funded. A total of $20,000. was awarded in total to the principal investigator at the University of Florida, and co-principal investigator at the University of South Carolina towards the research project.

Even with a nearly 11 month delay in the disbursement of startup funds, a decrease in requested funding of less than 9% of the requested budget, and the removal of the contract monitor within NASA Langley, the research team was made unusually strong progress towards the completion of the research outlined in this proposal.

Motivation

The effective utilization of many large scale numerical simulators requires an interactive capability to judge validity of the model chosen as well as the accuracy and efficiency of the solution procedures applied. Using their best scientific judgment, the scientist must be able to rapidly modify simulations for improvement in the fidelity of simulations, or to effect design changes in a collaborative environment. Performing this work on remote parallel machines poses special problems which must be resolved for effective utilization of these resources in meaningful applications. Historically, a diverse collection of parallel computational techniques have been developed for a wide class of multiprocessor hardware in order to iteratively solve systems of linear equations

associated with structural analysis, to approximate solutions of coupled design optimization problems, or to obtain time accurate solutions of aerodynamic flows over complex aerospace vehicle geometries. However, to enable simultaneous or collective use of these tools by different analysts in different laboratories, via virtual environments that necessarily operate over networks, it is absolutely imperative that a number of as yet unsolved technical barriers must be overcome.

Summary of Accomplishments:

The first year of research completed a focused plan of research that specifically addressed such technical barriers;

1. Originally designed specifically for the Intel Paragon architecture, the tracking and steering controller library (Kaulgud, A. and R.C. Sharpley. 1995. An Interactive Tracking/Steering Library. IMI Report 95:10. Department of Mathematics, University of South Carolina, Columbia, SC (Aug.)) was ported by project personnel to the general message passing language MPI (W. Gropp, E. Lusk and A. Skjellmun, USING MPI, Portable Parallel Programming with the Message-Passing Interface. The MIT Press, Cambridge, 1995.) for use with massively parallel MIMD machines.

2. Additional improvements were made to network code components of the tracking/steering library to permit secure use of the library through firewalls. This was tested using a fluid flow in porous media model (for a description, see L. Scott Johnson, A. Kaulgud, R.C. Sharpley, R.E. Ewing, Z. Leyk, J. Pasciak, M. Celia, and J.R. Brannan, Integration of Contaminant Transport Simulators on Parallel Machines with a Graphical User Interface for Remote Interactive Modeling, in Proceedings of the 1997 Simulation Multiconference," Atlanta, April 1997, Soc. for Computer Simulation International, San Diego.) over the vBNS network between the University of South Carolina and Texas A&M University.

3. The researchers continued to extend their earlier contributions to multiresolution and wavelet analysis to derive, develop and implement wavelet-based methodologies for the compression, transmission, decoding and visualization of multidimensional finite element logically rectangular geometry and simulation data in a networked environment. The wavelet library WV was further refined, incorporating encoding algorthims including the bitstream encoder of Gao, et al (Z. Gao, A. Andreev and R.C. Sharpley, Data Compression and Elementary Encoding of Wavelet Coefficients, IMI Report 97:02, Department of Mathematics, University of South Carolina, Columbia, SC (Jan. 97)).

On-line documentation of WV and a web-based demo of application codes for data compression and feature extraction are respectively available at

http://www.math.sc.edu/~sjohnson/wvlib/
http://www.math.sc.edu/~sjohnson/wvlib/demo/

4. The research team extended its methodologies for handling other classes of simulation data over network environments. These efforts included the development of multiwavelet, divergence free formulations amenable for the compression and transmission of flow field simulations as discussed in

Multiwavelets and Particle Image Velocimetry Methods, A. Kurdila, O. Rediniotis, T. Strganac, J. Ko, *40th Structures, Dynamics, and Materials Conference*, AIAA Paper Number AIAA-99-1309.

5. The research team has likewise extended its applications of multiresolution-based simulation methods to include reduced order model representations of dynamical systems appearing in classical aeroelastic studies. In this paradigm, low dimensional models are derived via multiresolution and wavelet methods from classical, high-dimensional FEM models of coupled fluid-structural interaction problems. The low order models enable the possiblitity of network simulation and real-time transmission of simulation results to remote sites for evaluation by engineers. The technical results are summarized in the publication

Multiresolution Methods for Reduced Order Models for Dynamical Systems, A. Kurdila, C. Prazenica, O. Rediniotis, T. Strganac, *40th Structures, Dynamics, and Materials Conference*, AIAA Paper Number AIAA-99-1263.

The details of these latter two contributions discussed in (4) and (5) above are included in the technical attachments.

Appendix (I)

Multiwavelets and Particle Image Velocimetry Methods, A. Kurdila, O. Rediniotis, T. Strganac, J. Ko, *40th Structures, Dynamics, and Materials Conference*, AIAA Paper Number AIAA-99-1309.

Multiwavelets and Particle Image Velocimetry Methods

Andrew J. Kurdila*
Department of Aerospace Engineering, Mechanics, and Engineering Science,
University of Florida, Gainesville, Florida 32611-6

Othon Rediniotis*, Thomas Strganac§, Jeonghwan Ko†
Department of Aerospace Engineering,
Texas A&M University, College Station, Texas 77843-3141

Abstract

In recent work the authors multilevel filtering for the analysis of digital Particle Image Velocimetry (PIV) based on multiresolution analysis. The essential contribution of this work was twofold. We sought to demonstrate the feasibility and amenability of wavelet based methods for local filtering and cross correlation calculations required in PIV methods. This work focussed on the derivation of windowed cross-correlation expressions for wavelet-based expansions that are not orthogonal (or biorthogonal) over the cross-correlation window. The methodology makes use of recently introduced "refinable functions" and generalized connection coefficients derived in wavelet-based finite element methods. In addition, we sought to develop divergence-free bases for flow modeling and order reduction. This paper extends these recent developments by deriving multiwavelet constructions applicable for the analysis of PIV. In contrast to our previous work, (1) the techniques herein make use of multiple scaling functions, (2) the local cross-correlations do not require "boundary modifications" that are computationally expensive, (3) the derived wavelet-based multiresolutions are orthogonal over the interrogation window, and (4) the same multiwavelets yield constructions of simple divergence free bases suitable for order reduction.

(1) Review and Motivation

To motivate the derivation of wavelet-based PIV algorithms that follow, we briefly review the methodology derived in Ref. 26. Frequently, instantaneous planar velocity distributions are derived from two captured images, separated by a known time interval, by cross-correlating corresponding sampling windows in the two images. In typical approaches[3], the image data from a window (for a 512x512 image, a typical window size is 32x32 pixels) taken in the first image and that from a window at the same position in the second image are cross-correlated. Consider the two consecutive images. We let $f(k,l)$ and $g(k,l)$ represent the pixel intensities (typically 0-255) at pixel locations (k,l) in the first and second images, respectively. From any of a number of texts (see for example, Shapiro and Rosenfeld[21]) treating digital image processing, we find that the discrete *normalized* cross-correlation $R(m,n)$ associated with discrete functions $f(k,l)$ and $g(k,l)$ is given by:

$$R(m,n) = \frac{\sum_k \sum_l f(k,l) g(k+m, l+n)}{\sum_k \sum_l f^2(k,l) \sum_k \sum_l g^2(k,l)} = \frac{\tilde{R}(m,n)}{\|f\|^2 \|g\|^2} \tag{1}$$

In this expression, the function $R(m,n)$ measures the correlation of the discrete functions $f(k,l)$ and $g(k,l)$ when they are relatively shifted by (m,n) pixels. We do not explicitly express the limits of summation, as this will clearly depend on the window size and location. The location of the cross-correlation peak gives the mean displacement of the particles in the interrogation window. This process is repeated by moving the window, until the entire image is covered. In Ref. 3, inaccuracies are introduced by the fact that the window in the second image is at the same location as the window in the first image. This could yield erroneous predictions since some of the particles in the first window could, due to their finite velocity, move outside of the interrogation window. The likelihood of erroneous predictions of the particle displacement grows as the flow velocity or, equivalently, the displacement increases. Moreover, the successful performance of the cross-correlation

*Associate Professor, Member AIAA
†PostDoctoral Research Associate, Member AIAA
§Associate Professor, Fellow Member AIAA

requires the use of a rather large interrogation window, typically 32x32 pixels. The algorithm returns a single velocity prediction for the entire interrogation window, therefore, all of the points within the window are assumed to have the same uniform velocity, and any spatial velocity gradients within the window are missed altogether. This restriction, can be somewhat alleviated by overlapping the interrogation windows. In general, for a 512x512 image, the velocity map has a grid size of 16x16. This resolution is inadequate when fine length scales are to be resolved. The determination of a local maxima is clearly difficult without significant filtering.

As shown in detail in Ref. 26, it is possible to derive an expression for the windowed *un-normalized* cross-correlation for functions in 1D expressed in terms of wavelet expansions as

$$\tilde{R}_{\Omega}(2^{-J}\xi) = \sum_{k}\sum_{l}\sum_{m=0}^{w} f_k g_l \Gamma^{0,0}_{k-s-m,l-\xi-s-m} \tag{2}$$

where the coefficients $\Gamma^{0,0}_{s,t}$ are the so-called connection coefficients, or refinable integrals. In two dimensions, the cross-correlation becomes

$$\begin{aligned}\tilde{R}_{\Omega}(2^{-J}\xi_1,2^{-J}\xi_2) &= \sum_{k,n}\sum_{l,o}\sum_{m,p}^{w_1,w_2} f_{k,n} g_{l,o} \Gamma^{0,0}_{k-s_1-m,l-\xi_1-s_1-m} \Gamma^{0,0}_{n-s_2-p,o-\xi_2-s_2-p} \\ &= \sum_{l,o} g_{l,o}\left(\sum_{k,n}\sum_{m,p}^{w_1,w_2} f_{k,n} \Gamma^{0,0}_{k-s_1-m,l-\xi_1-s_1-m} \Gamma^{0,0}_{n-s_2-p,o-\xi_2-s_2-p}\right) \\ &= \sum_{l,o} g_{l,o} M(l-\xi_1-m, o-\xi_2-s_2-p)\end{aligned} \tag{3}$$

We note the following :

(i) The integrals defining $\Gamma^{0,0}_{s,t}$ are not trivial to calculate in general. For many cases of interest, the wavelet scaling functions ϕ comprising the integrals cannot be expressed in closed form.

(ii) Numerical methods exist for calculating the entries $\Gamma^{0,0}_{s,t}$ to any degree of precision. Techniques for evaluating these integrals are discussed in Ref. 23 and Ref. 24.

(iii) Once the entries of $\Gamma^{0,0}_{s,t}$ have been calculated numerically, they can be stored and applied very rapidly. The number of nonzero entries in $\Gamma^{0,0}_{s,t}$ is proportional to the length of the mask defining the wavelet.

(iv) The entries of $\Gamma^{0,0}_{s,t}$ are different for different (families of) wavelets.

The expressions for the wavelet-based local cross-correlations in equations (2) and (3) allow local wavelet filtering, and the development of multilevel methods. As an example, the performance of these multilevel algorithms is summarized in Figures (1) - (9), which show that the multilevel filtering can be effective in improving the fidelity of cross-correlation calculations. For example, Figures (1) - (4) show that local cross correlations can be recursively calculated to improve local maximum identification using the multilevel algorithms described in Ref. 26. If the simple multilevel filtering algorithm (zero-pass coarse, all-pass details) depicted in Figure (5) is employed, highly accurate velocity fields can be reconstructed as depicted in Figures (6)-(9).

Still, the cross correlation expressions in equations (2) and (3) are obviously more complicated to implement than the conventional cross-correlation depicted in equation (1). Simply put, the complexity of the former expressions can be attributed to the fact that the selected (Daubechies compactly supported) wavelets employed in Ref. 26 are not orthogonal over the interrogation window. In this paper, we derive new classes of multiwavelets that are indeed orthogonal over the interrogation window. With these new classes of wavelets and filters, the calculations required to implement wavelet-based PIV methods are greatly simplified. Tables (1) and (2) list the newly derived filters corresponding to the orthogonal multiwavelets developed precisely for local interrogation windows.

Finally, it has been shown in Ref. 27 that divergence-free wavelet bases derived from the work in Ref. (28),(29),(30) can provide the foundation for order reduction methods applicable to incompressible flows. We conclude this paper by deriving divergence-free multiwavelets from the same underlying orthonormal multiwavelets used in the multilevel filtering operations described above.

(2) Multiwavelets and Multiresolution Analysis

The essential difference between the methodology introduced in this paper, and the earlier work by the authors in Ref. 26, 27 is that we make use of a collection of r real-valued, scalar functions to generate the multiresolution. In vector form, the scaling functions (or generators) and wavelet functions are denoted

$$\Phi(x) \stackrel{\Delta}{=} \begin{Bmatrix} \phi^1(x) \\ \vdots \\ \phi^r(x) \end{Bmatrix} \quad \Psi(x) \stackrel{\Delta}{=} \begin{Bmatrix} \psi^1(x) \\ \vdots \\ \psi^r(x) \end{Bmatrix}$$

Carefully note that the superscript denotes the specific generator in a family of generators. The translates and dilates of the scaling functions and wavelets are given by

$$\Phi_{j,k}(x) = \begin{Bmatrix} \phi^1_{j,k}(x) \\ \vdots \\ \phi^r_{j,k}(x) \end{Bmatrix} \quad \Psi_{j,k}(x) = \begin{Bmatrix} \psi^1_{j,k}(x) \\ \vdots \\ \psi^r_{j,k}(x) \end{Bmatrix}$$

In these equations we have introduced the usual shorthand notation

$$f_{j,k}(x) = 2^{j/2} f(2^j x - k)$$

Each vector of scaling functions and wavelets satisfies a matrix two scale relationship, shown below.

$$\Phi(x) = \sum_k \sqrt{2}[a_k]\Phi(2x-k)$$

$$\Psi(x) = \sum_k \sqrt{2}[b_k]\Phi(2x-k)$$

$$\Phi_{j,k}(x) = \sum_s [a_s]\Phi_{j+1,2k+s}(x)$$

$$\Psi_{j,k}(x) = \sum_s [b_s]\Phi_{j+1,2k+s}(x)$$

In this paper, we will deal with orthonormal families of multiwavelets. Specifically, we will employ a family of multiwavelets derived in Ref. 35 using the intertwining techniques described in Ref. 34. The requirements that the multiple scaling functions and multiple wavelets defined above are orthonormal manifests itself as conditions on the matrix masks. The requirement that the generators and wavelets are orthonormal to themselves is easily derived from the identities

$$\int_R \Phi(x)\Phi^T(x-k)dx = \delta_{0,k} \cdot I$$

$$\int_R \Psi(x)\Psi^T(x-k)dx = \delta_{0,k} \cdot I$$

Upon expansion, we have

$$\int_R \sum_s \sqrt{2}[a_s]\Phi(2x-s)\sum_m \Phi^T(2x-2k-m)\sqrt{2}[a_m]^T dx$$

$$= \sum_{m,s} \sqrt{2}[a_s]\int_R \Phi(2x-s)\Phi^T(2x-2k-m)dx\sqrt{2}[a_m]^T$$

$$= \sum_{m,s} 2[a_s]\delta_{0,2k+m-s}[a_m]^T = 2\delta_{0,k} \cdot I$$

Hence, the masks defining the generators and the wavelets must satisfy

$$\sum_m 2[a_{2k-m}][a_m]^T = 2\delta_{0,k} \cdot I$$

$$\sum_m 2[b_{2k+m}][b_m]^T = 2\delta_{0,k} \cdot I$$

In addition, we require that the generators and wavelets define (orthogonal) complementary spaces. That is, the generators are orthogonal to the wavelets on any fixed level.

$$\int_R \Phi(x)\Psi^T(x-k)dx = 0$$

When we expand these expressions, we obtain

$$\int_R \sum_s \sqrt{2}[a_s]\Phi(2x-s)\sum_m \Phi^T(2x-2k-m)\sqrt{2}[b_m]^T dx = 0$$

$$\sum_{m,s} \sqrt{2}[a_s]\int_R \Phi(2x-s)\Phi^T(2x-2k-m)dx\sqrt{2}[b_m]^T = 0$$

Thus, the generators will be orthogonal to the wavelets on the same level provided that the masks satisfy

$$\sum_m [a_{2k+m}][b_m]^T = 0$$

The specific set of orthonormal multiwavelets considered in this paper are depicted in Figures (14) and (15). Their matrix masks are summarized in Tables (1) and (2).

For the derivation that follows in the next section, we will likewise have occasion to interpret the wavelet identities above in terms of the Z transform. If $[h_n]$ $n = \cdots -2,-1,0,1,2,\cdots$ is a sequence of matrices, the formal Z transform of the sequence is defined to be

$$H(z) = \sum_{n \in Z} [h_n] z^{-n}$$

Sometimes we simply refer to this as the frequency domain representation of the sequence $[h_n]$ $n = \cdots -2,-1,0,1,2,\cdots$. In any of a number of standard texts, it is shown that wavelets can be interpreted as a two channel filter bank depicted in Figure (16). The two channel filter bank is comprised of a cascade of convolution, upsampling and downsampling operators. It is not difficult to show that the mapping from input to output in the

two channel filter bank depicted in Figure (16) can be derived as

$$y_1(z) = \tfrac{1}{2}\left[H(z)X(z) + H(-z)X(-z)\right]$$
$$y_2(z) = \tfrac{1}{2}\left[G(z)X(z) + G(-z)X(-z)\right]$$
$$\begin{aligned}\tilde{x} &= \tilde{H}y_1 + \tilde{G}y_2 \\ &= \tfrac{1}{2}\{\tilde{H}(z)H(z)X(z) + \tilde{H}(z)H(-z)X(-z) \\ &\quad + \tilde{G}(z)G(z)X(z) + \tilde{G}(z)G(-z)X(-z)\} \\ &= \tfrac{1}{2}\{\tilde{H}(z)H(z) + \tilde{G}(z)G(z)\}X(z) \\ &\quad + \tfrac{1}{2}\{\tilde{H}(z)H(-z) + \tilde{G}(z)G(-z)\}X(-z)\end{aligned}$$

Conditions that are sufficient to guarantee that the input to the filter bank exactly matches the output of the filter bank can be seen by inspection to be

$$\tilde{H}(z)H(z) + \tilde{G}(z)G(z) = 2I(z^{-1})$$
$$\tilde{H}(z)H(-z) + \tilde{G}(z)G(-z) = 0$$

These two conditions are referred to as the perfect reconstruction, and alias-canceling conditions, repsectively. A two channel filter bank that satisfies these conditions defines a family of biorthogonal multiwavelets and their associated multiresolution analyses.

(3) Simple Divergence-Free Multiwavelets

As shown in Ref. 27, divergence free wavelets can be employed in many postprocessing tasks associated with particle image velocimetry. During numerical experiments carried out in Ref. 27, it was found that the treatment of finite domains typically encountered in digital PIV image processing proved to be particularly troublesome. In this section, we show that a very simple modification of the methodology suggested in Ref. 33 yields families of divergence free multiwavelets. The construction is trivial, in fact, if we are given an original orthonormal multiwavelet basis system.

Suppose we are given the orthonormal multiple scaling functions and wavelets as discussed in Section (2). In this case, it is trivial to show that the derivatives of the generators satisfy a two scale relationship of their own.

$$\Phi_-(x) = \Phi'(x) = \sum_k 2\sqrt{2}\left[a_k\right]\Phi'(2x-k)$$
$$\Phi_-(x) = \sum_s \sqrt{2}\left[a_{-,s}\right]\Phi_-(2x-s)$$

where the new set of masks are defined to be

$$\left[a_{-,s}\right] = +2\left[a_s\right]$$

Similarly, we can define candidate multi-wavelets as

$$\Psi_-(x) = \sum_s \sqrt{2}\left[b_{-,s}\right]\Phi_-(2x-s)$$

where

$$\left[b_{-,s}\right] = +2\left[b_s\right]$$

It is important to note that the candidate functions $\Phi_-(x), \Psi_-(x)$ above do not constitute an orthonormal system of scaling functions and generators. In a similar fashion, we can construct candidate multiple scaling functions and wavelets by integrating the original orthonormal generators and wavelets. In this case, the associated two scale relations can be written as

$$\Phi_+(x) = \sum_k \sqrt{2}\left[a_{+,k}\right]\Phi_-(2x-k)$$

$$\Psi_+(x) = \sum_k \sqrt{2}\left[b_{+,k}\right]\Phi_+(2x-k)$$

where

$$\left[a_{+,k}\right] = \tfrac{1}{2}\left[a_k\right]$$
$$\left[b_{+,k}\right] = \tfrac{1}{2}\left[b_k\right]$$

Again, we emphasize that the multiple set of scaling functions $\Phi_+(x), \Psi_+(x)$ do not constitute an orthonormal set of multiwavelets. However, the two sets of functions $\left(\Phi_-(x), \Psi_-(x)\right)$ and $\left(\Phi_+(x), \Psi_+(x)\right)$ do constitute a set of biorthogonal multiwavelets. This is easily seen by observing that the Z-transform of the masks associated with each of these pairs of functions satisfies

$$A_+(z) = +\tfrac{1}{2}A(z) \qquad B_+(z) = +\tfrac{1}{2}B(z)$$
$$A_-(z) = +2A(z) \qquad B_-(z) = +2B(z)$$

As a consequence, we have

$$A_+(z)A_-(z^{-1})^T = (+\tfrac{1}{2}A(z))(+2A(-z)^T) = A(z)A(-z)^T = I$$
$$B_+(z)B_-(z^{-1})^T = (+\tfrac{1}{2}B(z))(+2B(-z)^T) = B(z)B(-z)^T = I$$
$$A_+(z)B_-(z^{-1})^T = (+\tfrac{1}{2}A(z))(+2B(-z)^T) = A(z)B(-z)^T = 0$$
$$B_+(z)A_-(z^{-1})^T = (+\tfrac{1}{2}B(z))(+2A(-z)^T) = B(z)A(-z)^T = 0$$

However, the above set of equations simply guarantees that the two channel filter bank associated with the differentiated functions

$\Phi_-(x), \Psi_-(x)$ and the integrated functions $\Phi_+(x), \Psi_+(x)$ satisfy the perfect reconstruction and anti-aliasing conditions derived in Section (2).

From these observations, it is relatively simple, although algebraically tedious, to construct simple divergence free bases. While the details exceed the scope of this short note, a multiresolution analysis comprised of divergence free multiwavelets can be constructed in terms of the primal bases

$$\bar{\psi}_{(1,0),2} = \begin{Bmatrix} -\psi_-(x)\phi(y) \\ \psi(x)\phi_-(y) \end{Bmatrix}$$

$$\bar{\psi}_{(0,1),1} = \begin{Bmatrix} \phi_+(x)\psi(y) \\ -\phi(x)\psi_+(y) \end{Bmatrix}$$

$$\bar{\psi}_{(1,1),2} = \begin{Bmatrix} -\psi_+(x)\psi(y) \\ \psi(x)\psi_-(y) \end{Bmatrix}$$

and their respective dual bases

$$\bar{\theta}_{(1,0),2} = \theta_{(1,0),2}e_2 = \begin{Bmatrix} 0 \\ \psi(x)\phi_-(y) \end{Bmatrix}$$

$$\bar{\theta}_{(0,1),1} = \theta_{(0,1),1}e_1 = \begin{Bmatrix} \phi_-(x)\psi(y) \\ 0 \end{Bmatrix}$$

$$\bar{\theta}_{(1,1),2} = \theta_{(1,1),2}e_2 = \begin{Bmatrix} 0 \\ \psi(x)\psi_-(y) \end{Bmatrix}$$

The reader should carefully note that we have suppressed the superscript denoting the specific generator (or wavelet) in the list of multiple generators (or wavelets). That is, each basis appearing on the right hand side of these equations should have a superscript that runs between 1... r.

However, with this notational convention, we can succinctly state the multiresolution decomposition of divergence free subspaces of the square integrable functions as

$$\text{Each } \bar{f} \in (L_2(R))^2 \cap \{\bar{f}: \operatorname{div}\bar{f} = 0\}$$

$$\bar{f} = \sum_{j\in Z}\sum_{e\in E^*}\sum_{i\neq j,k\in Z\times Z} \begin{Bmatrix} \langle \theta_{e,i,j,k}, f_1 \rangle \bar{\psi}_{e,i,j,k}(x,y) \\ \langle \theta_{e,i,j,k}, f_2 \rangle \bar{\psi}_{e,i,j,k}(x,y) \end{Bmatrix}$$

Again, for notational simplicity, it is understood that the above summations are carried out over all the specific elements of the r-vectors of generators and multiwavelets.

Conclusions:

In this paper, we have reviewed recent work by the authors that derive (I) multilevel filtering methods and (ii) reduced order divergence-free bases in terms of orthonormal, and biorthogonal wavelets, respectively. It was noted that the first set of algorithms for multilevel filtering could be expensive to implement because the selected wavelet bases are not orthogonal over the interrogation window. In the second set of algorithms, a biorthogonal basis system was employed that is unrelated to the orthonormal system employed for multilevel filtering. In this paper, we summarize a set of orthonormal multiwavelets that have been derived via intertwining techniques to address these deficiencies. In short, the derived multiwavelet bases (i) are orthogonal over the PIV interrogation window, (ii) yield fast, local cross-correlation calculations that are amenable to multilevel implementations, and (iii) can be used to derive simple divergence free bases for incompressible flow modeling order reduction. Algorithmic implementation and performance are discussed in a forthcoming paper.

References:

1. Grant, I. and Liu, A., 'Method for the Efficient Incoherent Analysis of Particle Image Velocimetry Images', Applied Optics, Vol. 28, No. 10, pp. 1745-1748, May 1989.

2. Keane, R. D. and Adrian, R. J., 'Theory of Cross-Correlation Analysis of PIV Images', Applied Scientific Research, Vol. 49, pp. 191-215, 1992.

3. Willert, C. E. and Gharib, M., 'Digital Particle Image Velocimetry', Experiments in Fluids, Vol. 10, pp. 181-193, 1991.

4. Shimada, H., Murata, S., and Kise, H., 'Particle Image Velocimetry Based on Fourier Transform Method for Measurement of Fluctuating Velocity Fields', Trans. JSME, Vol. 58, No.552, pp. 2472-2478, 1992.

5. Grant, I., and Qiu, J.H., 'Digital Convolution Filtering Techniques on an Array Processor for Particle Image Velocimetry', Applied Optics, Vol. 29, No.29, pp. 4327-4329, October 1990.

6. Nakatani, N. and Oshio, T., 'Processing PTV Patterns by Holographic Correlation Technique', Proceedings of the Seventh International

Symposium on Flow Visualization, pp. 746-751, 1995.

7. Arnold, W. and Hinsch, K., 'Purely Optical Parallel Processing in Particle Image Velocimetry and the Study of Flow Structures', ICALEO '88, Optical Methods in Flow and Particle Diagnostics, Proc. Laser Institute of America Vol. 67, pp. 157-165, 1988.

8. Farrell, P. V. and Goetsch, D., 'Optical Analysis of Particle Image Velocimetry Data', ICALEO '89, Optical Methods in Flow and Particle Diagnostics, Proc. Laser Institute of America Vol. 68, pp. 82-91, 1989.

9. Coupland, J. M. and Halliwell, N. A., 'Particle Image Velocimetry: Rapid Transparency Analysis Using Optical Correlation', Applied Optics, Vol. 27 No. 10, pp. 1919-1921, May 1988.

10. Grant, I. and Liu, A., 'Directional Ambiguity Resolution in Particle Image Velocimetry by Pulse Tagging', Experiments in Fluids, Vol. 10, pp. 71-76, 1990.

11. Adrian, R. J., 'Image Shifting Technique to Resolve Directional Ambiguity in Double Pulsed Velocimetry', Applied Optics, Vol. 25, No. 21, pp. 3855-3858, November 1986.

12. Landreth, C. C., Adrian, R. J., and Yao, C. S., 'Double Pulsed Particle Image Velocimeter with Directional Resolution for Complex Flows', Experiments in Fluids, Vol. 6, pp. 119-128, 1988.

13. Grobel, M. and Merzkirch, W., 'White-Light Speckle Velocimetry Applied to Plane Free Convective Flow', Experimental Heat Transfer, Vol. 4,pp. 253-262, 1991

14. Landreth, C. C. and Adrian, R. J., 'Electrooptical Image Shifting for Particle Image Velocimetry', Applied Optics, Vol. 27, No.20, pp. 4216-4220, October 1988.

15. Trump, D. D., Goss, L. P., and Gogineni, S. P., 'Two-Color Particle Image Velocimetry Employing a Color CCD Camera', Proceedings of the Seventh International Symposium on Flow Visualization, pp. 622-627, 1995.

16. Gilarranz, J., Singh, K., Ko, J., Rediniotis, O., and Kurdila, A., 'High Frame-Rate, High Resolution Cinematographic Particle Image Velocimetry', AIAA Paper No. 97-0495, 35th Aerospace Sciences Meeting & Exhibit, Reno, NV., January, 1997.

17. Vogel, A., and Lauterborn, W., 'Time Resolved Particle Image Velocimetry', Optics and Lasers in Engineering, Vol. 9, pp. 274-294, 1988.

18. Chui, C.K., editor, 'Wavelets: A Tutorial in Theory and Applications', Academic Press, New York, 1992.

19. Mallat, S., 'A Theory for Multiresolution Signal Decomposition: The Wavelet Representation', IEEE Transactions on Pattern Analysis and Machine Intelligence, Vol. 11, No. 7, pp. 674-693, July 1989

20. DeVore, R. A and Lucier, B. J., 'Image Compression Through Wavelet Transform Coding', IEEE Transactions on Information Theory, Special Issue on Wavelet Transforms and Multiresolution Signal Analysis, Vol. 38, No. 2, pp. 719-746, March 1992.

21. Shapiro, L. G. and Rosenfeld, A., 'Computer Vision and Image Processing', Academic Press, Boston, 1992.

22. Daubechies, I., 'Ten Lectures on Wavelets', SIAM, Philadelphia, PA, 1992

23. Dahmen, W. and Micchelli, C.A., 'Using the Refinement Equation for evaluating Integrals of Wavelets', SIAM Journal of Numerical Analysis, Vol. 30, pp. 507-537, 1993.

24. Latto, A., Resnikoff, H. L. and Tenenbaum, E., 'The Evaluation of Connection Coefficients of Compactly Supported Wavelets', Aware Inc., Technical Report No. AD910708, 1991.

25. Ko, J., Kurdila, A. J., and Pilant, M. S., 'A Class of Finite Element Methods Based on Orthonormal, Compactly Supported Wavelets', Computational Mechanics, Vol. 16, pp. 235-244, 1995.

26. Ko, J. Kurdila, A.J., Gilarranz, J. and Rediniotis, O., "Particle Image Velocimetry via Wavelet Analysis," AIAA Journal, Vol. 36, No. 8, August, 1998.

27. Ko, J., Kurdila, A.J., and Rediniotis, O., "Divergence Free Bases and Multiresolution Methods for Reduced Order Flow Modeling," *AIAA Journal*, in review.

28. Lemarie-Rieusset, P., "Ondelettes Vecteurs a Divergence Nulle," *C.R. Acad. Sci. Paris*, t. 313, Serie I, 1991, pp. 213-216.

29. Lemarie-Rieusset, P., "Wavelets, Splines and Divergence-Free Vector Functions," *in Approximation Theory, Spline Functions and Applications*, pp. 381-390, Kluwer Academic Publishers, 1992.

30. Lemarie-Rieusset, P., "Un Theoreme d'Inexistence Pour les Ondelettes Vecteurs a Divergence Nulle," *C.R. Acad. Sci. Paris*, t. 319, Serie I, p. 811-813, 1994.

31. Urban, K., "On Divergence-Free Wavelets," *Advances in Computational Mathematics*, Vol. 4, No. 1, 1995, pp. 51-82.

32. Urban, K., "Using Divergence Free Wavelets for the Numerical Solution of the Stokes Problem," in *Algebraic Multilevel Iterations*, Axelsson, O., and Polman, B. (eds.), Nijmegen, pp. 259-278, 1996.

33. Lakey, J.D., Massopust, P.R., and Pereyra, M.C., "Divergence-Free Multiwavelets", *preprint*, 1998.

34. Donovan, G.C., Geronimo, J.S., and Hardin, D.P., "Intertwining multiresolution analyses and the construction of piecewise-polynomial wavelets," *SIAM Journal of mathematical analysis*, Vol. 27, No. 6, 1996, pp. 1791-1815.

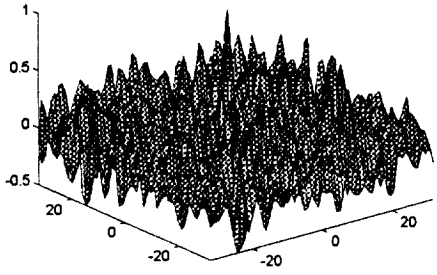

Figure (1) Cross correlation, for multilevel algorithms : Denoising on multiple decompositions, 2 level details, Ref. 26

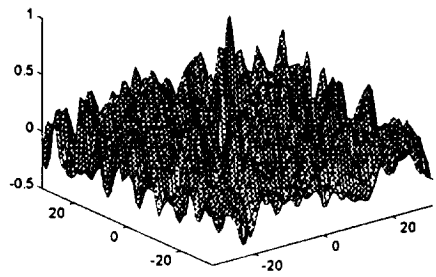

Figure (2) Cross correlation, for multilevel algorithms : Denoising on multiple decompositions, 3 level details, Ref. 26

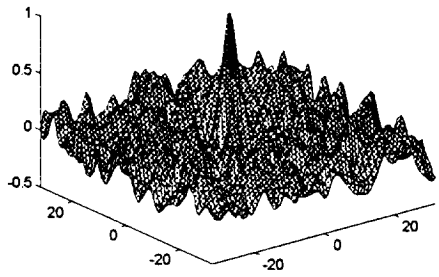

Figure (3) Cross correlation, for multilevel algorithms : Denoising on multiple decompositions, 4 level details, Ref. 26

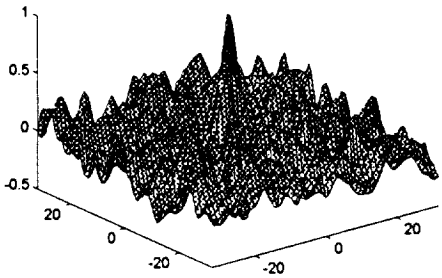

Figure (4) Cross correlation, for multilevel algorithms : Denoising on multiple decompositions, 5 level details, Ref. 26

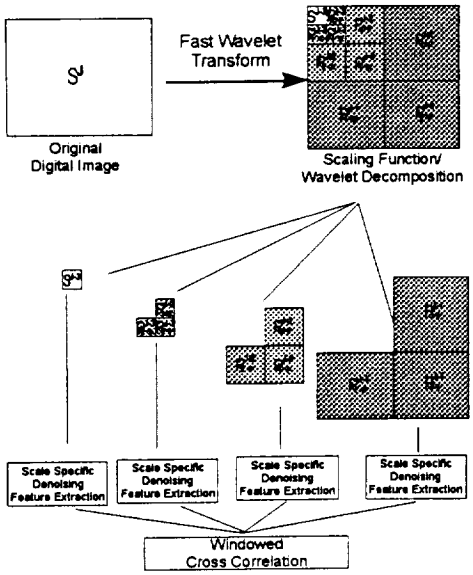

Figure (5) Multilevel Decomposition and Filtering Schematic, Ref. 26

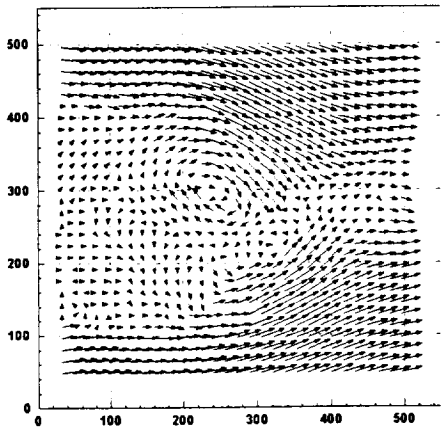

Figure (6) Consecutively collected frames, velocity reconstruction via multilevel wavelet algorithms, t=0 sec, Ref. 26

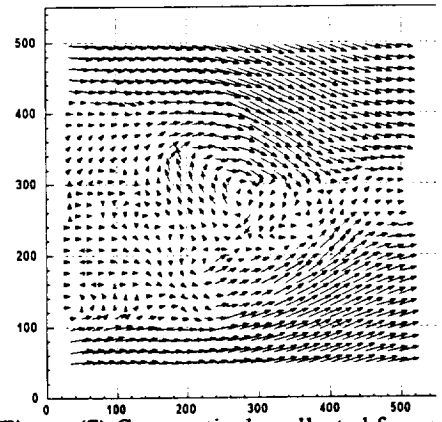

Figure (7) Consecutively collected frames, velocity reconstruction via multilevel wavelet algorithms, t=1 sec, Ref. 26

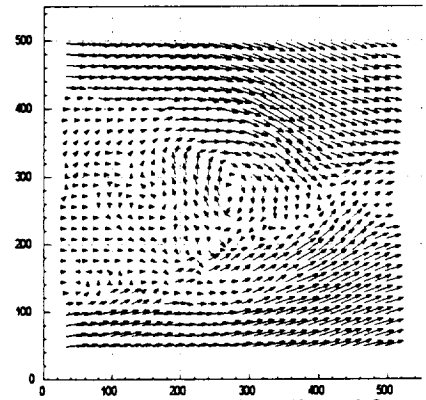

Figure (8) Consecutively collected frames, velocity reconstruction via multilevel wavelet algorithms, t=2 sec, Ref. 26

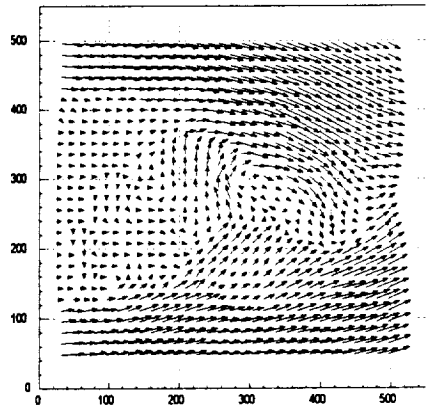

Figure (9) Consecutively collected frames, velocity reconstruction via multilevel wavelet algorithms, t=3 sec, Ref. 26

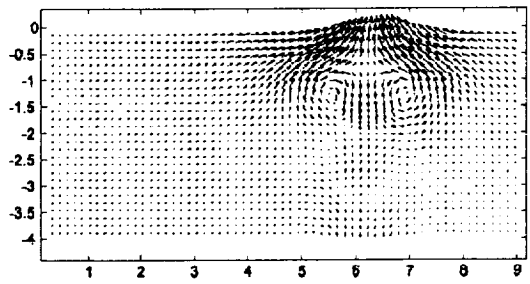

(a) Original POD Mode 2, 61 x 27

Figure (10) Proper orthogonal decomposition Mode 2, Ref. 27

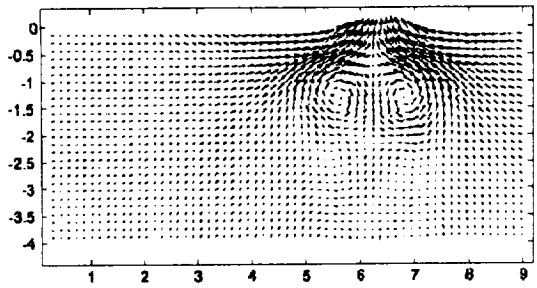

(b) First Compression, POD Mode 2, 480

Figure (11) Proper orthogonal decomposition, Mode 2, omit 1st level details, Ref. 27

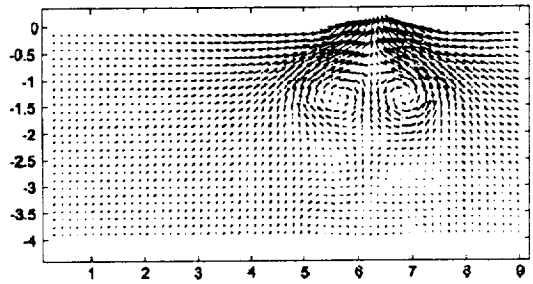

(c) Second Compression, POD Mode 2, 153

Figure (12) Proper orthogonal decomposition, Mode 2, omit 1st + 2nd level details, Ref. 27

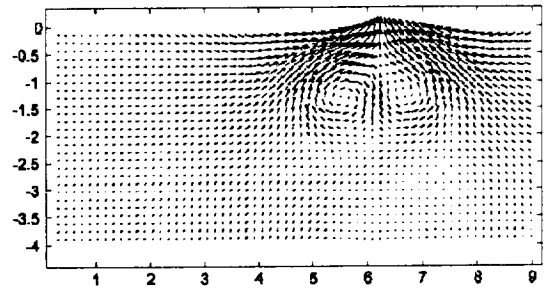

(d) Third Compression,, POD Mode 2 60

Figure (13) Proper orthogonal decomposition, Mode 2, multiscale filter, omit 1st +2nd + 3rd level Ref. 27

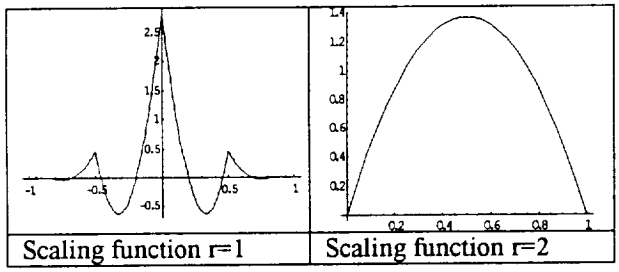

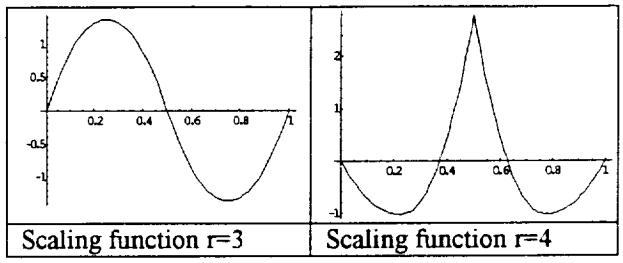

Figure (14) Orthonormal Multiwavelet scaling functions, Ref. 35

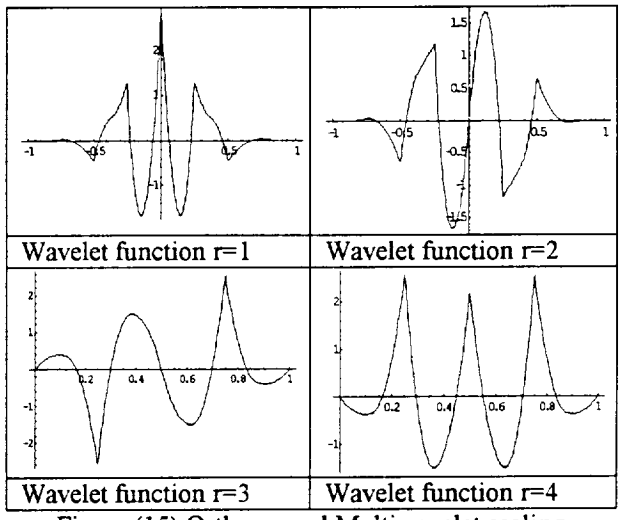

Figure (15) Orthonormal Multiwavelet scaling functions, Ref. 35

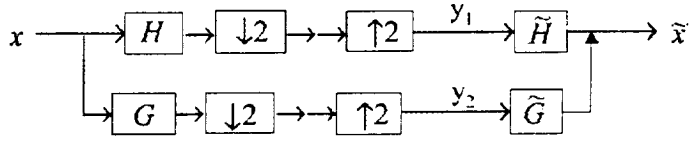

Figure (16) Prototypical two channel filter bank

n	$[a]_n$
-	$\begin{pmatrix} 0 & .0163446406689 & -.0342630216987 & -.0327571725062 \\ 0 & 0 & 0 & 0 \\ 0 & 0 & 0 & 0 \\ 0 & 0 & 0 & 0 \end{pmatrix}$
-	$\begin{pmatrix} .113474174186 & .0163446406689 & -.42217244289 & -.236881317738 \\ 0 & 0 & 0 & 0 \\ 0 & 0 & 0 & 0 \\ 0 & 0 & 0 & 0 \end{pmatrix}$
C	$\begin{pmatrix} .707106781187 & .0163446406689 & .422172442 & -.236881317738 \\ 0 & .618718433538 & -.220970869121 & -.0988211768803 \\ 0 & .707106781187 & 0 & 0 \\ 0 & -.338665211381 & -.316332942563 & -.201862521835 \end{pmatrix}$
1	$\begin{pmatrix} .113474174186 & .0163446406689 & .0342630216987 & -.0327571725062 \\ .342326598441 & .618718433538 & .220970869121 & -.0988211768803 \\ 0 & -.707106781187 & 0 & 0 \\ .699272287923 & -.338665211381 & .316332942563 & -.201862521835 \end{pmatrix}$

Table (1) Matrix masks for multi-scaling function filters

I	$[b]_n$
-	0 - .034263021699 .032757172499 0 - .048455229972 .046325637623 0 0 0 0 0 0 0 0
-	.113474174186 - .42217244289 .23688131774 .160476716113 - .597041994395 .335000772219 0 0 0 0 0 0 0 0
(	.707106781187 - - .23688131774 0 .618718433538 -.220970869121 - 0 0 -.288675134594 -.645497224366 0 .018873165380 -.316332942563 .551430926265
:	.113474174186 - - .032757172499 .160476716113 .023114812506 .048455229972 - 0 0 -.288675134591 .645497224363 .539276980493 .018873165379 -.223959608744 .551430926253

Table (2) Matrix masks for multi-wavelet function filters

Appendix (II)

Multiresolution Methods for Reduced Order Models for Dynamical Systems, A. Kurdila, C. Prazenica, O. Rediniotis, T. Strganac, *40th Structures, Dynamics, and Materials Conference*, AIAA Paper Number AIAA-99-1263.

MULTIRESOLUTION METHODS FOR REDUCED ORDER MODELS FOR DYNAMICAL SYSTEMS

A. Kurdila*, C. Prazenica*, O. Rediniotis† and T. Strganac†

*Department of Aerospace Engineering,
Mechanics, and Engineering Science
University of Florida
Gainesville, Florida 32611-6250

† Department of Aerospace Engineering
Texas A&M University
College Station, TX 77843-3141

Abstract

This paper derives reduced order input-output models for a class of nonlinear systems by utilizing wavelet approximations of kernels appearing in Volterra series representations. While Volterra series representations of nonlinear system input/output have been understood from a theoretical standpoint for some time, their practical use has been limited owing to the dimensionality of approximations of the higher order (nonlinear) terms. In general, wavelet and multiresolution analysis have shown considerable promise for the compression of signals, images and, most importantly for this paper, some integral operators. Unfortunately, causal Volterra series representations are expressed in terms of integrals that are restricted to products of half-spaces, and there is a significant difficulty in deriving wavelets that are appropriate for Volterra kernel representations (i.e., that are restricted to semi-infinite domains). In addition, it is necessary to derive Volterra kernel expansions that are consistent with the method of sampling used to obtain input and output data. This paper derives discrete approximations for truncated Volterra series representations in terms of a specific class of biorthogonal wavelets. When employing a zero order hold for both the input and output signals, it is shown that a consistent approximation of the input/output system is achieved for a specific choice of biorthogonal wavelet families. This family is characterized by the fact that all of the wavelets are biorthogonal with respect to the characteristic function of the dyadic intervals employed to define the zero order hold. It is also simple to show that an arbitrary choice of wavelet systems will not, in general, provide a consistent approximation for arbitrary input/output mappings. Numerical studies of the derived methodologies are carried out using experimental pitch-plunge response data from the TAMU Nonlinear Aeroelastic Testbed.

Introduction

A large collection of methods have been investigated for obtaining reduced order representations of linear and nonlinear dynamical systems in structural mechanics, fluid mechanics, aeroelasticity and control theory. These methods include such diverse strategies as modal synthesis, Ritz vector reduction, rational approximation, Hankel approximation and proper orthogonal decomposition (POD). In fluid mechanics, the study of the underlying qualitative dynamics of various classes of flows using POD has been carried out in [24,26]. In these studies, the essential goal is often to study the topological dynamics underlying the more complex model [26, 25, 24]. Sometimes, the ultimate goal is the development of control experiments or methodologies [38]. In structural mechanics, Ritz basis reduction methods denoted "component mode synthesis" have emerged as a distinct discipline [see Craig, 1981]. Order reduction methods designed to preserve the fidelity of specific measurements, observations or performance functionals have been studied in linear control theory [see Skelton, 1983]. Similarly, some researchers have employed reduced basis methods in the simulation and control of the nonlinear Navier-Stokes equations [30,27,28]. More

recently, component mode synthesis methods have been studied for a class of open loop simulations of aeroelastic systems [40].

One common feature of most of these methods is that they are not directly amenable to online updating or adaptive "response subspace" selection strategies. For example, the authors have shown that geometrically nonlinear control methods can be extremely effective in some applications to nonlinear aeroelastic control [41]. These strategies rely on an accurate reduced order model of the nonlinear open loop dynamics. At the same time, the authors have shown that some POD reduced basis methods can be extremely effective in generating low-dimensional approximations of uncontrolled flow. As an example, the authors have studied the efficiency of POD methods for obtaining reduced order models of synthetic jets in [38]. The performance of this approach for studying a particular response regime is discussed in detail in [38]. By including the four POD modes, three of which are depicted in Figures (1) through (3), 99% of the total energy of the flow is captured by the reduced order Navier-Stokes simulation, as shown in Figure (4).

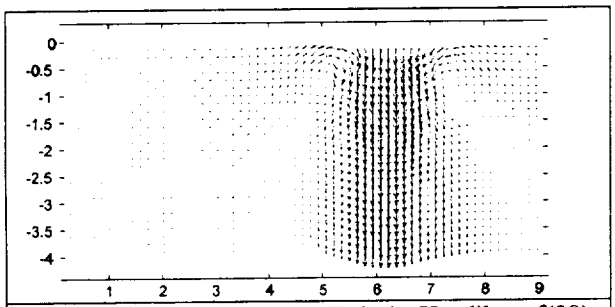

Figure 1: POD Mode 1, Rediniotis, Kurdila, ref(38)

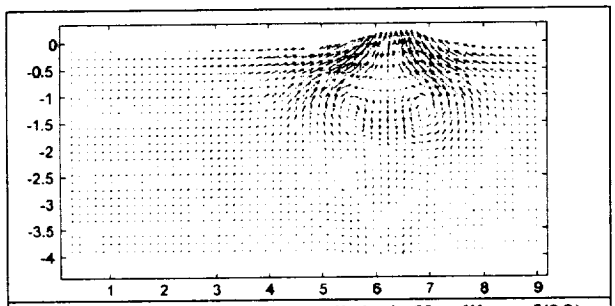

Figure 2: POD Mode 2, Rediniotis,Kurdila, ref(38)

We emphasize that this study considers an *uncontrolled* response regime. The difficulty, however, is not associated with producing a single reduced order model that captures the essential dynamics of a particular operating or flow regime. Rather, if the overall goal of the model order reduction is to enable control of the system, the reduced order model must be accurate over

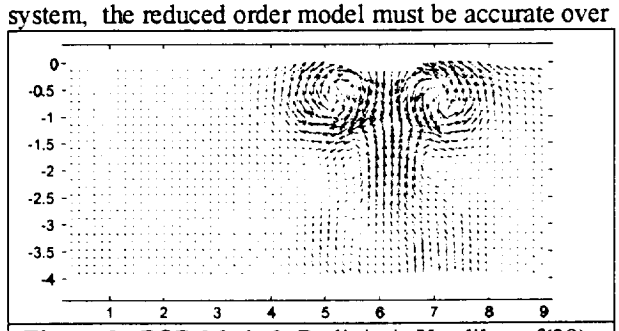

Figure 3: POD Mode 3, Rediniotis,Kurdila, ref(38)

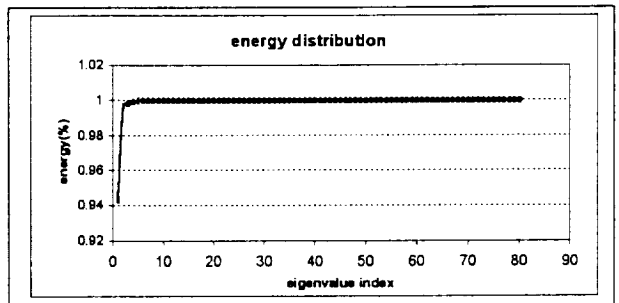

Figure 4: %Energy retained in reduced POD basis simulation, Rediniotis & Kurdila, ref(38)

a diverse family of response regimes. In other words, because the express purpose of control is to alter (usually drastically) the system dynamics, any model derived from the response history of the open loop, uncontrolled system may be a very poor approximation for the closed loop system dynamics. This fact is well understood, and well documented, in the control theory and linear system theory literature [see for example, Skelton 1983 and the references therein]. Unfortunately, the problem is compounded in many applications to aeroelasticity or fluid mechanics in that the governing Navier-Stokes equations are inherently nonlinear. Some of the richest theory available for treating order reduction problems have been derived in the context of linear system theory.

In this paper, we present a methodology that is directed precisely towards achieving efficient reduced order representations of a class of nonlinear systems that is amenable to adaptive and online control methodologies. If we acknowledge that the underlying dynamics are nonlinear *a priori*, a reasonable starting point is to choose one of the standard nonlinear system parameterizations. Possible choices include Fliess functional expansions, Chen series or Volterra series. Silva in [43] studies the identification of Volterra series from impulse response for aeroelastic applications. We will consider the identification of similar systems, but for general input/output histories.

Volterra Operators and Approximation

In this paper, we will consider those dynamical systems expressed in terms of Volterra integral operators, and restrict our attention to single-input/single-output systems. The output y(t) can be written formally as the infinite sum

$$y(t) \overset{\Delta}{=} y_1(t) + y_2(t) + y_3(t) + \ldots \tag{1}$$

where each term $y_i(t)$ is the output of the i^{th} order Volterra integral operator. For i=1 or i=2, we have

$$y_1(t) = \int_{-\infty}^{t} h_1(t-\xi)u(\xi)d\xi \tag{2}$$

$$y_2(t) = \int_{-\infty}^{t}\int_{-\infty}^{t} h_2(t-\xi, t-\eta)u(\xi)u(\eta)d\xi d\eta \tag{3}$$

where the input is u(t). The theoretical foundations of the Volterra series in equation (1), sufficient conditions for its convergence and the form for higher order terms can be found in [42]. In this paper, we are concerned only with the first and second (i=1,i=2) order terms of the Volterra series.

Now, we introduce the characteristic function $\chi(t)$ of the unit interval [0,1]

$$\chi(t) = \begin{cases} 1 & t \in [0,1] \\ 0 & \text{otherwise} \end{cases} \tag{4}$$

and its scaled and dilated translates

$$\begin{aligned} \chi_{j,k}(t) &\overset{\Delta}{=} 2^{j/2}\chi(2^j t - k) \\ &= \begin{cases} 2^{j/2} & 2^j t - k \in [0,1] \quad k2^{-j} \le t \le (k+1)2^{-j} \\ 0 & \text{otherwise} \end{cases} \end{aligned} \tag{5}$$

We can obtain a zero-order hold approximation of the input by writing

$$u(t) \overset{\Delta}{=} \sum_k u_{j,k}\chi_{j,k}(t) \tag{6}$$

After some tedious algebra, it is shown in [39] that the zero order hold approximation of both the first and second order kernels of the Volterra series is simply

$$y_{j,n} = \sum_{s=n-1}^{0} h_{1,j,s}u_{j,n-s-1} + \sum_{r=n-1}^{0}\sum_{s=n-1}^{0} h_{2,(r,s)}u_{j,n-r-1}u_{j,n-s-1} \tag{7}$$

where

$$\begin{aligned} h_{1,j,m} &\overset{\Delta}{=} 2^{j/2}\int_{m2^{-j}}^{(m+1)2^{-j}} h_1(s)ds \\ h_{2,(r,s)} &\overset{\Delta}{=} 2^{j/2}\cdot 2^{j/2}\int_{r2^{-j}}^{(r+1)2^{-j}}\int_{s2^{-j}}^{(s+1)2^{-j}} h_2(\xi,\eta)d\xi d\eta \end{aligned} \tag{8}$$

Thus far, we have shown that the zero order hold for both input and output induces the discrete Volterra Series in equations (7) and (8). We now show that the discrete integrals in equation (8) are amenable to wavelet induced multilevel approximation. Suppose that the first order kernel h_1 is approximated as

$$h_1(\xi) = \sum_p h_{1,j,p}\varphi_{j,p}(\xi) \tag{9}$$

where the only assumption on the functions $\varphi_{j,p}$ at this point is that they are dual to $\chi_{j,m}$ in the sense that

$$\int \varphi_{j,p}\chi_{j,m} = \delta_{p,m} \tag{10}$$

The first order term in equation (7) becomes

$$\begin{aligned} y_{1,j,n} &= \sum_k \int_0^{\infty}\left(\sum_p h_{1,j,p}\varphi_{j,p}(s)\right)\chi_{j,n-k-1}(s)ds\cdot u_{j,k} \\ y_{1,j,n} &= \sum_k\sum_p h_{1,j,p}\int_0^{\infty}\varphi_{j,p}(s)\chi_{j,n-k-1}(s)ds\cdot u_{j,k} \end{aligned} \tag{11}$$

which can be rewritten as

$$\begin{aligned} y_{1,j,n} &= \sum_k h_{1,j,n-k-1}u_{j,k} \\ y_{1,j,n} &= \sum_s h_{1,j,s-1}u_{j,n-s} \end{aligned} \tag{12}$$

Likewise, if we approximate the second order kernel as

$$\begin{aligned} h_2(\xi,\eta) &= \sum_{r,s} h_{2,j,(r,s)}\varphi_{j,(r,s)}(\xi,\eta) \\ &= \sum_r\sum_s h_{2,j,(r,s)}\varphi_{j,r}(\xi)\varphi_{j,s}(\eta) \end{aligned} \tag{13}$$

and substitute this kernel in equation (8), we recover, for the second order term in equation (7)

$$\begin{aligned} y_{2,j,n} &= \sum_{k,m}\int_0^{\infty}\int_0^{\infty}\left(\sum_r\sum_s h_{2,j,(r,s)}\varphi_{j,r}(\xi)\varphi_{j,s}(\eta)\right) \\ &\qquad \chi_{j,n-k-1}(\xi)\chi_{j,n-m-1}(\eta)d\xi d\eta\cdot u_{j,k}u_{j,m} \\ y_{2,j,n} &= \sum_{k,m,r,s} h_{2,j,(r,s)}\delta_{(r,s),(n-k-1,n-m-1)}u_{j,k}u_{j,m} \\ y_{2,j,n} &= \sum_{k,m} h_{2,j,(n-k-1,n-m-1)}u_{j,k}u_{j,m} \\ y_{2,j,n} &= \sum_{s,p} h_{2,j,(s,p)}u_{j,n-s-1}u_{j,n-p-1} \end{aligned} \tag{14}$$

Indeed, equations (12) and (14) illustrate that, so long as the approximating family is biorthogonal with respect to the characteristic functions $\chi_{j,m}$, we obtain the discrete input and output Volterra Series derived in equations (7) and (8) by a zero order hold of input and output. In the next section, we discuss the specific selection of a biorthogonal wavelet basis to achieve the desired approximation order and order reduction.

Biorthogonal Wavelet Approximations

In the last section, we showed that a consistent approximation of the discrete Volterra input - output mapping is achieved when kernel approximates are selected to be biorthogonal with respect to characteristic functions of dyadic intervals. In this section we discuss a class of biorthogonal wavelets that satisfy this condition and induce a multilevel approximation of the Volterra kernels. Recall that a multiresolution analysis is a nested sequence of spaces $\{V_k\}_{k\in Z}$

$$\cdots V_{-1} \subset V_0 \subset V_1 \subset V_2 \cdots \tag{15}$$

where V_0 is the span of the translates of a fixed function φ.

$$V_0 = \underset{k\in Z}{Span}\{\varphi(x-k)\} \tag{16}$$

In this equation, Z is the collection of (signed) integers. The remaining spaces in the sequence of equation (15) are defined by dilation. We define

$$\varphi_{j,k}(x) = 2^{j/2}\varphi(2^j x - k) \tag{17}$$

and subsequently

$$V_j = \underset{k\in Z}{Span}\{\varphi_{j,k}\} \tag{18}$$

If we have a second multiresolution $\{\widetilde{V}_k\}_{k\in Z}$ generated by the function $\widetilde{\varphi}$, we say that the pair $\{V_k\}_{k\in Z}$ and $\{\widetilde{V}_k\}_{k\in Z}$ form a biorthogonal multiresolution provided that

$$\langle \varphi_{j,k}, \widetilde{\varphi}_{j,m} \rangle = \int_R \varphi_{j,k}(x)\widetilde{\varphi}_{j,m}(x)dx = \delta_{k,m} \tag{19}$$

A wavelet ψ is a function whose dilates and translates span the complement spaces W_j defined via

$$V_{j+1} = V_j + W_j \tag{20}$$

so that

$$W_j = \underset{k\in Z}{Span}\{\psi_{j,k}\} \tag{21}$$

where

$$\psi_{j,k}(x) \overset{\Delta}{=} 2^{j/2}\psi(2^j x - k) \tag{22}$$

A similar definition holds for the dual wavelet $\widetilde{\psi}$. As discussed in [31], it is possible to define dual wavelets ψ and $\widetilde{\psi}$ associated with the biorthogonal multiresolution analyses $\{V_k\}_{k\in Z}$ and $\{\widetilde{V}_k\}_{k\in Z}$ that satisfy

$$\langle \psi_{k,j}, \widetilde{\psi}_{m,n} \rangle = \delta_{(k,j),(m,n)} \tag{23}$$

In particular, this can hold if we find masks $\{a_k\},\{b_k\},\{\widetilde{a}_k\}$ and $\{\widetilde{b}_k\}$ that satisfy the two scale relationships:

$$\begin{aligned} \varphi(t) &= \sqrt{2}\sum_k a_k \varphi(2t-k) \\ \widetilde{\varphi}(t) &= \sqrt{2}\sum_k \widetilde{a}_k \widetilde{\varphi}(2t-k) \\ \psi(t) &= \sqrt{2}\sum b_k \varphi(2t-k) \\ \widetilde{\psi}(t) &= \sqrt{2}\sum \widetilde{b}_k \widetilde{\varphi}(2t-k) \end{aligned} \tag{24}$$

where

$$\begin{aligned} b_k &= (-1)^k \widetilde{a}_{-k+1} \\ \widetilde{b}_k &= (-1)^k a_{-k+1} \end{aligned} \tag{25}$$

If equations (24) and (25) are satisfied, fast multilevel algorithms can be derived that project a function onto various nested spaces. If $f \in V_j$, then f has a representation

$$f = \sum_k \alpha_{j,k}\varphi_{j,k}(\xi) \tag{26}$$

via equation (18), or as

$$f = \sum_k \alpha_{j-1,k}\varphi_{j-1,k}(\xi) + \sum_k \beta_{j-1,k}\psi_{j-1,k}(\xi) \tag{27}$$

from equation (20). Given the coefficients $\alpha_{j,k}$ in equation (26), it is easy to show that we can find the coefficients $\alpha_{j-1,k}$ and $\beta_{j-1,k}$ in equation (27)

$$\alpha_{j-1,k} = \sum_n \tilde{a}_{n-2k}\alpha_{j,n}$$
$$\beta_{j-1,k} = \sum_n \tilde{\beta}_{n-2k}\alpha_{j,n} \tag{28}$$

As an example, we obtain

$$\begin{aligned}\left(f,\tilde{\varphi}_{j-1,m}\right) &= \alpha_{j-1,m} = \sum_k \alpha_{j,k}\left(\varphi_{j,k},\tilde{\varphi}_{j-1,m}\right)\\ &= \sum_k \alpha_{j,k}\left(\varphi_{j,k},\sum_s \tilde{a}_s\tilde{\varphi}_{j,2m+s}\right)\\ &= \sum_{k,s}\alpha_{j,k}\tilde{a}_s\delta_{k,2m+s}\\ &= \sum_k \tilde{a}_{k-2m}\alpha_{j,k}\end{aligned} \tag{29}$$

Equation (28) is the decomposition formula associated with the set of biorthogonal wavelets (φ,ψ) and $(\tilde{\varphi},\tilde{\psi})$. A reconstruction formula can likewise be derived that gives the fine scale coefficients in terms of the coarse scale.

$$\alpha_{j,m} = \sum_k \left(a_{m-2k}\alpha_{j-1,k} + b_{m-2k}\beta_{j-1,k}\right) \tag{30}$$

These expressions can be used to obtain a multilevel representation of the Volterra kernels. Assume that the first order Volterra kernel is expressed on the finest scale as

$$h_1(\xi) = \sum_p h_{1,j,p}\varphi_{j,p}(\xi) = \sum_p \alpha_{j,p}\varphi_{j,p}(\xi) \tag{31}$$

where

$$h_{1,j,p} = \int_0^{\infty} h_1(\xi)\chi_{j,p}(\xi)d\xi = \int_{k2^{-j}}^{(k+1)2^{-j}} h_1(\xi)d\xi = \alpha_{j,p} \tag{32}$$

That is, we have identified $\chi_{j,p} \equiv \varphi_{j,p}$. With a recursive application of equation (20), a multilevel expansion of the first order kernel is obtained.

$$\begin{aligned}h_1(\xi) = &\sum_p \alpha_{j_0,p}\varphi_{j_0,p}(\xi) + \sum_p \beta_{j_0,p}\psi_{j_0,p}(\xi)\\ &+\sum_p \beta_{j_1,p}\psi_{j_1,p}(\xi)\\ &+\sum_p \beta_{j_2,p}\psi_{j_2,p}(\xi)\\ &\vdots\\ &+\sum_p \beta_{j,p}\psi_{j,p}(\xi)\end{aligned} \tag{33}$$

$$h_1(\xi) = \sum_p \alpha_{j_0,p}\varphi_{j_0,p}(\xi) + \sum_{l=j_0,j}\beta_{l,p}\psi_{l,p}(\xi)$$

Similarly, if we define the tensor product scaling functions

$$\begin{aligned}\Phi^*(\xi,\eta) &= \varphi^*(\xi)\varphi^*(\eta)\\ \Phi(\xi,\eta) &= \varphi(\xi)\varphi(\eta)\end{aligned} \tag{34}$$

and the tensor product wavelets

$$\begin{aligned}\Psi^1(\xi,\eta) &= \varphi(\xi)\psi(\eta)\\ \Psi^2(\xi,\eta) &= \psi(\xi)\varphi(\eta)\\ \Psi^3(\xi,\eta) &= \psi(\xi)\psi(\eta)\\ \Psi^{1*}(\xi,\eta) &= \varphi^*(\xi)\psi^*(\eta)\\ \Psi^{2*}(\xi,\eta) &= \psi^*(\xi)\varphi^*(\eta)\\ \Psi^{3*}(\xi,\eta) &= \psi^*(\xi)\psi^*(\eta)\end{aligned} \tag{35}$$

we obtain the following single scale representation of the second order kernel

$$h_2(\xi,\eta) = \sum_{r,s}\alpha_{j,(r,s)}\Phi_{j,(r,s)}(\xi,\eta) \tag{36}$$

The corresponding two-scale expansion of the kernel is

$$\begin{aligned}h_2(\xi,\eta) = &\sum_{m,n}\alpha_{j-1,(m,n)}\Phi_{j-1,(m,n)}(\xi,\eta)\\ &+\sum_{m,n}\beta^1_{j-1,(m,n)}\Psi^1_{j-1,(m,n)}(\xi,\eta)\\ &+\sum_{m,n}\beta^2_{j-1,(m,n)}\Psi^2_{j-1,(m,n)}(\xi,\eta)\\ &+\sum_{m,n}\beta^3_{j-1,(m,n)}\Psi^3_{j-1,(m,n)}(\xi,\eta)\end{aligned} \tag{37}$$

The development of the multilevel representation of the (nonlinear) second order kernel bears close resemblance to equation (33). We refer the interested reader to the details of the implementation of the first and second order kernels in [39].

Numerical and Experimental Results

In a series of papers, the authors have derived, implemented and tested reduced order models for the prototypical nonlinear aeroelastic system depicted in Figure (5) on the next page. This system is comprised of a NACA0012 airfoil that is capable of undergoing large amplitude response in either the pitch or plunge degrees of freedom. Any reasonable representation of the response of this system is inherently *geometrically* nonlinear owing to the unique design of the carriage on which the airfoil is mounted. The details of the design, shown schematically in Figure (6), are described in detail in [41].

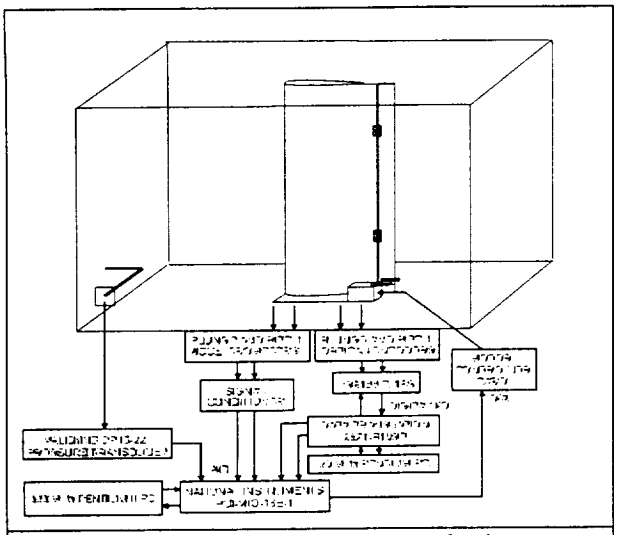

Figure 5: Prototypical nonlinear aeroelastic system

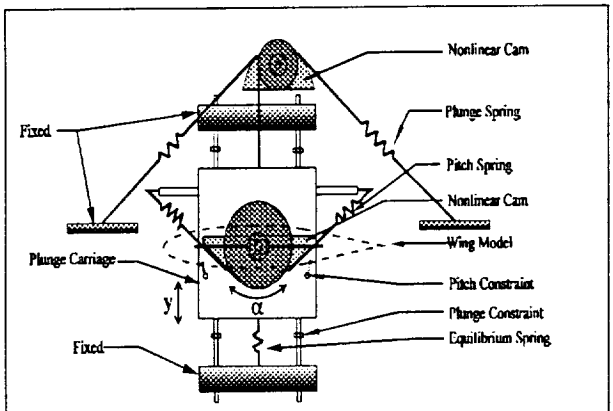

Figure 6: Carriage design

This system has been designed to exhibit large amplitude limit cycle oscillations in particular flow regimes, and the performance of geometrically nonlinear closed loop control methods is discussed in [41]. We note that a conventional representation of the nonlinear dynamics of this system, that was sufficiently accurate to derive closed loop flutter suppression control laws, was employed in these previous studies. It was comprised of two parametrically dependent, coupled nonlinear ordinary differential equations of second order. This is, perhaps, the simplest nonlinear model that could be used to represent the system. The pitch amplitude is so large that it may also be argued that stall effects likewise contribute significant nonlinear response that is not accounted for in the open loop model employed in [41]. In any event, in the current numerical example, we study the performance of the wavelet-based Volterra series system identification for this example. Angle encoders provide a measurement of the flap deflection as a function of time, which we take as input to the wavelet-based kernel identification algorithm. We choose the output to be the pitch angle, also measured by angle encoders as depicted in Figure (5), measured in radians. In this simple numerical experiment, we consider the experimental records from a single test in the identification process. The input measured flap deflection, output measured pitch and flow velocity in the tunnel are depicted in Figures (7), (8) and (9), respectively.

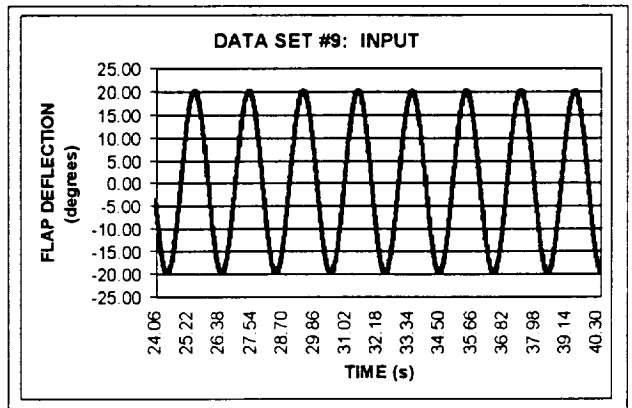

Figure 7: Experimental input – flap deflection

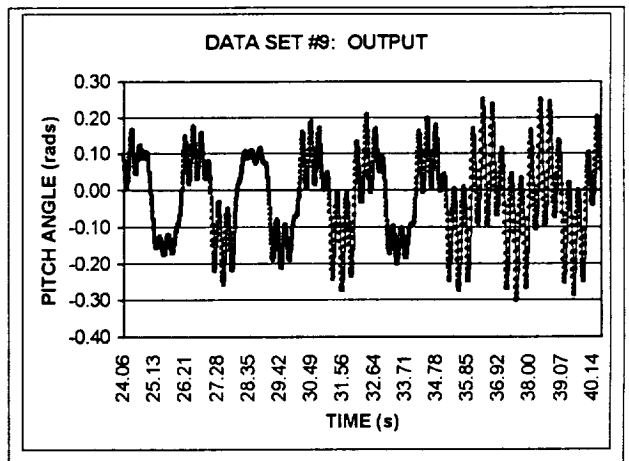

Figure 8: Experimental output – pitch angle

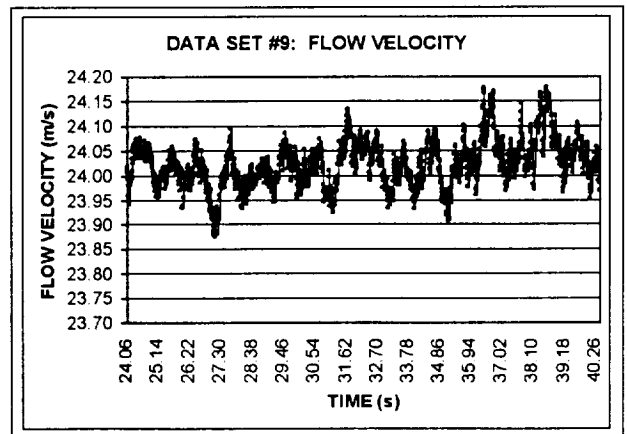

Figure 9: Flow velocity in the test section

It is important to note that this experimental data departs significantly from the framework presented in this paper. Specifically, the system is parametrically dependent on the flow velocity shown in Figure (9), which is clearly not constant. If we note that the flow velocity in the figure ranges between 23 and 24 m/s, it might be argued that the system is "nearly stationary" over the experiment. The implication is, of course, that the simple form of the Volterra kernels presented earlier are not applicable, strictly speaking. It is possible, however, to derive Volterra series expansions that are expressed in terms of time-dependent kernels. These expansions are applicable for a class of non-stationary systems, including the above-described system. We anticipate that the identified Volterra kernels should indeed vary parametrically with time for the system under consideration. The entire data set is comprised of 2048 sample points. Using a sliding window of 128 sample points, a weakly nonlinear Volterra series representation comprised of only the 1st order and 2nd order kernel was identified for the system. For this specific numerical test, the first order kernel was comprised of 4 terms, while the second order kernel was comprised of a 4 x 4 array. It should be noted that the 4 x 4 array is symmetric (see [42]), so that the cardinality of the Volterra series model is 4 + (5*4/2) = 14 terms. As shown in Figure (10), graph of the predicted output of the Volterra model is not discernible from the graph of the experimental output.

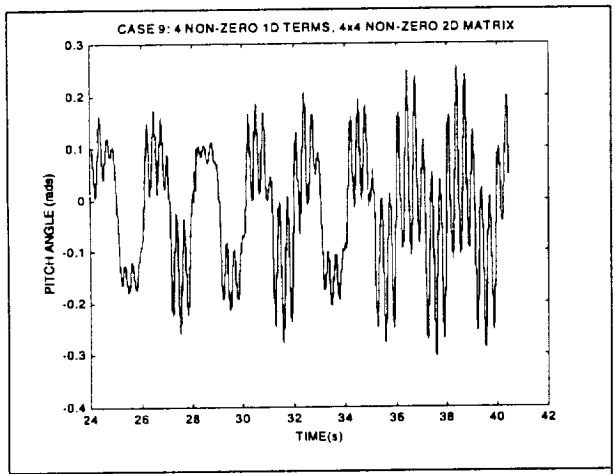

Figure 10: Graphs of predicted output from model identification and experimental output

Finally, the evolution of the kernels that comprise this non-stationary system can be appreciated by considering Figures (11) through (14). Figures (11) and (12) depict the representation of the Volterra kernels identified from the first and second sample windows of the identification process. Each is represented in terms of the same 14 basis functions, although it is clear that there is a slight variation between the sample windows that can be attributed to the non-stationary nature of the system under consideration.

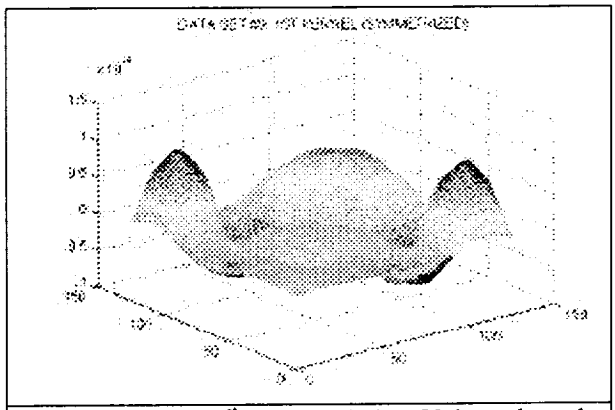

Figure 11: The 1st sample window Volterra kernel

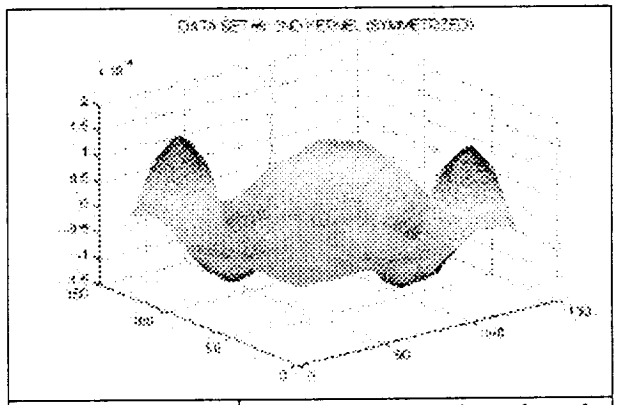

Figure 12: The 2nd sample window Volterra kernel

In comparison, the Volterra kernels identified for the 13th and 14th sample windows, while quite similar to one another, vary significantly from the Volterra kernels for the 1st and 2nd sample windows. Again, this is anticipated owing to the non-stationary character of the physical dynamical system.

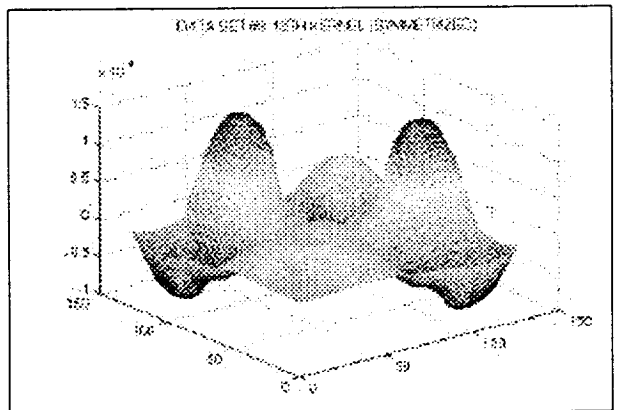

Figure 13: The 13th sample window Volterra kernel

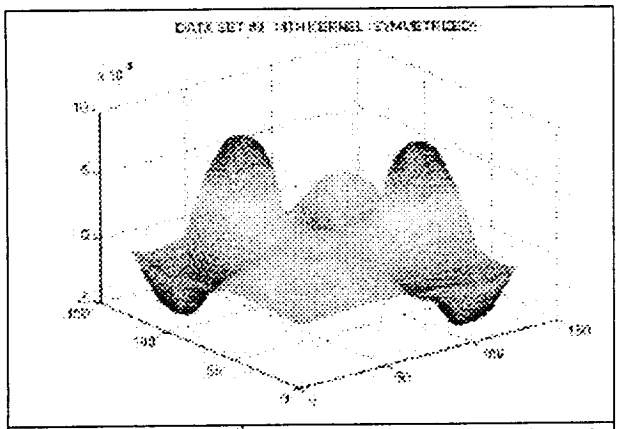

Figure 14: The 14th sample window Volterra kernel

Conclusions and Future Work

This paper has derived a wavelet and multiresolution based methodology for obtaining reduced order approximations of Volterra series. While Volterra series representations provide a succinct characterization of nonlinear system response in principle, their use has been limited in practice due to the large number of terms required to represent the higher order, nonlinear terms. We show that a consistent approximation of the Volterra input/output representation is achieved if two conditions are satisfied:
(1) a zero order hold is used for the input and output sequences, and
(2) a biorthogonal wavelet family is selected such that the generator is dual to characteristic functions that define the zero order hold.

The identification of a prototypical nonlinear aeroelastic system is studied to evaluate the potential of the derived method. The prototypical aeroelastic system undergoes large amplitude, limit cycle oscillations. The experimental data studied in the numerical examples is non-stationary, due to the non-negligible variations in wind tunnel velocity. Nevertheless, the wavelet identification of the nonlinear response was extremely accurate with the reduced order wavelet models. For a sample record size of 2048 data points and sliding window of 128 data points, the nonlinear response character was captured with as few as 14 wavelets. It was also shown that the nonlinear second order kernel did evolve in time, which is to be expected for the non-stationary nonlinear model. However, the variation in the nonlinear second order kernel was essentially slowly varying. One implication of the numerical tests is that the migration of these methodologies to on-line identification of Volterra kernels should be investigated immediately.

This paper suggests several subsequent lines of research. While the ability of the wavelet representations to compress integral operators was exploited implicitly, the methodology does not currently make use of the explicit multilevel structure that is available. For example, it is anticipated that multilevel and multigrid methods can be used to improve the convergence rate of the identification procedure. Essentially, the method would perform multiscale filtering of the input and output sequences a priori, before the kernels of the nonlinear kernel are estimated. The kernels themselves could then be estimated on resolutions that correspond to the filtered input and output sequences. Additionally, this paper also suggests that there should be a careful study of energy exchange in time-scale space for classical nonlinear dynamical systems of aeroelasticity. The structure of the kernels may be indicative of the time-frequency evolution of energy in the system. Finally, the identification procedure suggested in this paper is most useful when we can derive associated compensators for the nonlinear Volterra series. Such work has been studied in some classical texts, but the specific forms of the desired compensators for the multiresolution kernels have not been studied.

References

[1] Basseville, M., Benveniste, A., Chou, K.C., Golden, S.A., Nikoukhah, R. and Willsky, A., "Modeling and Estimation of Multiresolution Stochastic Processes," *IEEE Transactions on Information Theory*, Vol. 38, No. 2, March, 1992, pp. 766-784.

[2] Basseville, M., Benveniste, A. and Willsky, A.S., "Multiscale Autoregressive Processes, Part I: Schur-Levinson Parameterization," *IEEE Transactions on Signal Processing*, Vol. 40, No. 8, August, 1992, pp. 1915-1934.

[3] Benveniste, A., Nikoukhah, R. and Willsky, A.S., "Multiscale System Theory," *IEEE Transactions on Circuits and Systems*, Vol. 41, No. 1, January, 1994, pp. 2-15.

[4] Chou, K.C. and Willsky, A.S., "Kalman Filtering and Riccati Equations for Multiscale Processes," *Proceedings of the 29th Conference on Decision and Control*, Honolulu, Hawaii, December, 1990, pp. 841-846.

[5] Chou, K.C., Willsky, A.S. and Benveniste, A., "Multiscale Recursive Estimation, Data Fusion and Regularization," *IEEE Transactions on Automatic Control*, Vol. 39, No. 3, March, 1994, pp. 464-478.

[6] Chou, K.C., Willsky, A.S., Benveniste, A. and Basseville, M., "Recursive and Iterative

Estimation Algorithms for Multiresolution Stochastic Processes," *Proceedings of the 28th Conference on Decision and Control*, Tampa, Florida, December, 1989, pp. 1184-1189.

[7] Chou, K.C., Willsky, A.S. and Nikoukhah, R., "Multiscale Systems, Kalman Filters, and Riccati Equations," *IEEE Transactions on Automatic Control*," Vol. 39, No. 3, March, 1994, pp. 479-492.

[8] Nikolaou, M. and Mantha, D., "Efficient Nonlinear Modeling Using Wavelets and Related Compression Techniques," *AIChE Journal*, preprint.

[9] Nikolaou, M. and Vuthandam, P., "FIR Model Identification: Parsimony Through Kernel Compression with Wavelets," *AIChE Journal*, Vol. 44, No. 1, January, 1998, pp. 141-150.

[10] Palavajjhala, S., Motard, R.L. and Babu, J., "Process Identification Using Discrete Wavelet Transforms: Design of Prefilters," *AIChE Journal*, Vol. 42, No. 3, March, 1996, pp. 777-790.

[11] Tsatsanis, M.K. and Giannakis, G.B., "Time Varying System Identification and Model Validation Using Wavelets," *IEEE Transactions on Signal Processing*, Vol. 41, No. 12, December, 1993, pp. 3512-3523.

[12] Daubechies, I., "Orthonormal Bases of Compactly Supported Wavelets," *Communications on Pure and Applied Mathematics*, Vol. XLI, pp. 909-996, 1988.

[13] Chui, C.K., ed., *Wavelets: A Tutorial in Theory and Applications*, Academic Press, New York, 1992.

[14] Mallat, S., "A Theory for Multiresolution Signal Decomposition: The Wavelet Representation," *IEEE Transactions on Pattern Analysis and Machine Intelligence*, Vol. 11, No. 7, July 1989, pp. 674-693.

[15] DeVore, R. A. and Lucier, B. J., "Image Compression Through Wavelet Transform Coding," *IEEE Transactions on Information Theory, Special Issue on Wavelet Transforms and Multiresolution Signal Analysis*, Vol. 38, No. 2, pp. 719-746, March 1992.

[16] Jaffard, S., and Laurencot, P., "Orthonormal Wavelets, Analysis of Operators, and Applications to Numerical Analysis," in *Wavelets: A Tutorial in Theory and Applications* (Chui, C., ed.), pp. 543-601, Academic Press, San Diego, CA, 1992.

[17] Cortellezi, L, and Speyer, J., "Advance in Boundary Layer Control: Robust Reduced-Order Transition Controller" CAM Report 97-57.

[18] Loeve, M., "Functions Aleatoire de Second Ordre," *Compte Rend. Acad. Sci. (Paris)*, 1945.

[19] Karhunen, K., "Zur Spektral Theorie Stochasticher Prozesse," *Ann. Acad. Sci. Fennicae, Ser. A1, Math. Phys.*, 37, 1946.

[20] Lumley, J.L., "The Structure of Inhomogeneous Turbulent Flows," *Atmospheric Turbulence and Radio Wave Propagation* (ed. A.M. Yaglom and V.I. Tatarsky), p. 166, Moscow.

[21] Reichert, R.S., Hatay, F.F., Biringen, S. and Huser, A., "Proper Orthogonal Decomposition Applied to Turbulent Flow in a Square Duct," *Journal of Physics of Fluids*, Vol. 6, No. 9, pp. 3086-3092, September 1994.

[22] Ly, H.V., and Tran, H.T., "Proper Orthogonal Decomposition for Flow Calculations and Optimal Control in a Horizontal CVD Reactor," *Technical report*, Center for

[23] Tang, K.Y., Graham, W.R. and Peraire, J., "Active Flow Control Using a Reduced Order Model and Optimum Control," AIAA Paper ....., ...

[24] Aubry, N., Holmes, P., Lumley, J.L. and Stone, E., "The Dynamics of Coherent Structures in the Wall Region of a Turbulent Boundary Layer," Journal of Fluid Mechanics, Vol. 192, pp. 115-173, 1988.

[25] Ball, K.S., Sirovich, L. and Keefe, L.R., "Dynamical Eigenfunction Decomposition of Turbulent Channel Flow," *International Journal for Numerical Methods in Fluids*, Vol. 12, pp. 585-604, 1991.

[26] Berkooz, G., Holmes, P. and Lumley, J.L., "The Proper Orthogonal Decomposition in the Analysis of Turbulent Flows," *Annu. Rev. Fluid Mech.*, Vol. 25, pp. 539-575, 1993.

[27] Ito, K., and Ravindran, S.S., "Reduced basis method for flow control," *Technical report*, Center for research in scientific computation, North Carolina State University, 1997.

[28] Ito, K., and Ravindran, S.S., "A reduced basis method for control problems governed by PDEs," *Technical report*, Center for research in scientific computation, North Carolina State University, 1997.

[29] Ly, H.V., and Tran, H.T., "Proper Orthogonal Decomposition for Flow Calculations and Optimal Control in a Horizontal CVD Reactor," *Technical report*, Center for Research in Scientific Computation, North Carolina State University, 1997.

[30] Gunzburger, M.D., *Finite Element Methods for Viscous Incompressible Flows : a Guide to Theory, Practice, and Algorithms*, Academic Press, Boston, MA, 1989.

[31] Cohen, A., Daubechies, I. and Feauveau, J.-C., "Biorthogonal Bases of Compactly Supported

Wavelets," *Communications on Pure and Applied Mathematics*, Vol. XLV, pp. 485-560, 1992.

[32] Daubechies, I., *Ten Lectures on Wavelets*, SIAM, 1992.

[33] Lemarie-Rieusset, P., "Ondelettes Vecteurs a Divergence Nulle," *C.R. Acad. Sci. Paris*, t. 313, Serie I, p. 213-216, 1991.

[34] Lemarie-Rieusset, P., "Wavelets, Splines and Divergence-Free Vector Functions," *in Approximation Theory, Spline Functions and Applications*, pp. 381-390, Kluwer Academic Publishers, 1992.

[35] Lemarie-Rieusset, P., "Un Theoreme d'Inexistence Pour les Ondelettes Vecteurs a Divergence Nulle," *C.R. Acad. Sci. Paris*, t. 319, Serie I, p. 811-813, 1994.

[36] Urban, K., "On Divergence-Free Wavelets," *Advances in Computational Mathematics*, Vol. 4, No. 1, pp. 51-82, 1995.

[37] Urban, K., "Using Divergence Free Wavelets for the Numerical Solution of the Stokes Problem," in *Algebraic Multilevel Iterations*, Axelsson, O., and Polman, B. (eds.), Nijmegen, pp. 259-278, 1996.

[38] Rediniotis, O. K., Ko. J., Yue, X., and Kurdila, A.J., "Synthetic Jets, Their Reduced Order Modeling and Applications to Flow Control," AIAA Paper No., AIAA 99-1000, presented at the 37th Aerosciences Meeting and Exhibit, January, 1999, Reno, NV. Boston, 1993.

[39] Kurdila,A.J., Li, J., Liu, J. and Prazenica, C., "Reduced Order Representations of Volterra Series via Wavelet Expansions," preprint, January, 1999.

[40] Ko, J., Kurdila, A.J., and Strganac, T.W., "Nonlinear Control of a Prototypical Wing Section with Torsional Nonlinearity," *Journal of Guidance, Control, and Dynamics*, Vol. 20, No.6, Nov. 1997.

[41] Tang, D., Conner, M., and Dowell, E., "A Reduced Order Finite State Aerodynamic Model and Its Application to a Nonlinear Aeroelastic System," preprint, 1997.

[42] Schetzen, M., The Volterra and Wiener Theories of Nonlinear Systems, John Wiley & Sons, 1980.

[43] Silva, W., "Discrete Time Linear and Nonlinear Aerodynamic Impulse Responses for Efficient CFD Analyses," Ph.D. Dissertation, The College of William of Mary in Virginia, 1997.